

Study of the impact of 220 kV SISFCL on the distance protection for transmission line

YINGHONG LUO¹, TONGTONG SHI¹, LINKE HUANG²

¹ *School of Automation and Electrical Engineering
Lanzhoujiaotong University*

² *State Grid Gansu Economic Research Institute
Lanzhou 730070, China
e-mail: Sticker_T@163.com*

(Received: 07.09.2017, revised: 24.12.2017)

Abstract: As the most typical application of superconducting technology, the Saturated Iron core Superconducting Fault Current Limiter (SISFCL) is a kind of ideal high voltage limiter, which can achieve noticeable limiting endless stream and has wide application prospect. However, the selectivity and sensitivity of the distance protection (DP) in the high voltage transmission network would be affected by the impedance characteristics of SISFCL. For these problems, firstly the structure and the working principle of the SISFCL are introduced briefly. Secondly, the impact mechanisms of 220 kV SISFCL on the original distance protection for the transmission line (TL) are analyzed. Then two methods of eliminating influences are deduced from the previous analysis and an improved setting method based on SISFCL for distance protection is proposed. Finally, we used EMTDC/PSCAD software to build the 220 kV SISFCL and distance protection model in the transmission network. The simulation results demonstrate that the proposed setting strategy can effectively improve the selectivity and sensitivity of distance protection and provide a reference for the practical applications of SISFCL applied to the transmission line.

Key words: SISFCL, distance protection, EMTDC/PSCAD, 220 kV transmission line, setting method

1. Introduction

With the increase of capacity of the power system and the expansion of interconnected power grids, the needs of growing demand for power load, improvements in power quality and reduction cost of power delivery have been fulfilled. However on the other side, all these achievements have contributed to short-circuit current increases sharply at the same time [1–4].

The increase in short-circuit current has put forward rigorous demands in the dynamic and thermal stability of some equipment in the primary side of the power system. And the short-circuit current level of some nodes in the power system exceeded the circuit breaker interrupting

limit [5–7], which has given rise to a serious threat to the safe operation of the power system. Thus, it is an urgent problem to suppress the short-circuit current of the system imminently [8, 9].

With the continuous development of superconducting technology, the Saturated Iron core Superconducting Fault Current Limiter (SISFCL) exhibits low impedance in steady-state, the impedance changes rapidly when the fault occurs, high impedance in current limit state, under control during the entire current limiting process. With these advantages, the SISFCL has gradually caught the attention of industry and academia. Some scholars predict that the 220 kV SISFCL is the most commonly used application in the future of SFCL market. Certain some engineering test prototypes have been developed in China [10–12]. At present, most of the main protection and backup protection of 220 kV TL in China have DP. In the current limiting process, the SISFCL acts as a large reactance which contributes to adverse impacts on the original DP of the TL. The combination method of impedance circle characteristic offset, proposed by [13], significantly eliminates the influences of the solid state fault limiter on the DP. In [14], the improvement measures of the DP successfully eliminate the influence of resistance type SFCL on single-phase grounding DP. However, these two methods cannot be implemented to the SISFCL for impedance varies with the current. The PC-protection algorithm proposed in [15] needs to calculate the SISFCL impedance in real time, which is sometimes difficult to realize in engineering applications.

In this paper, DP and SISFCL studies are based on the 220 kV TL. Firstly, the models of the DP, TL and SISFCL are established in the PSCAD software. Then, the current limiting performances of short-circuit current at the different fault points and the SISFCL are analyzed. Furthermore, the influence of the SISFCL on TLDP is intensively studied and a DP setting method for eliminating this kind of influence is proposed. Finally, the proposed setting method is simulated and verified.

2. The principle of SISFCL and distance protection

2.1. The structure and working principle of SISFCL

The three-phase structure of the 220 kV SISFCL shown in Fig. 1. The DC excitation system is shared by three-phase, and composed of the superconducting magnet immersed in liquid nitrogen, a quick break switch, energy release resistance and DC power supply. Each single-phase of AC is composed of two adjacent AC windings which immersed in insulating oil.

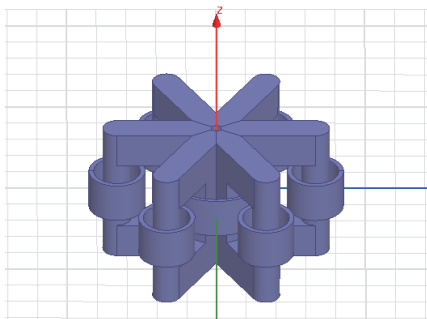


Fig. 1. Schematic structure of three-phase SISFCL

The fast-switch is in a closed state when the TL with SISFCL is running normally. The DC power supplies the superconducting magnet so that the right (left) iron core is in the forward (reverse) depth saturation. Fig. 2(a), (H_{R0}, Ψ_{R0}) is a steady state saturation point of the right side iron core. The integrated flux linkage of the right iron core is $\Psi_R(t)$, which is generated by the current of AC and DC winding.

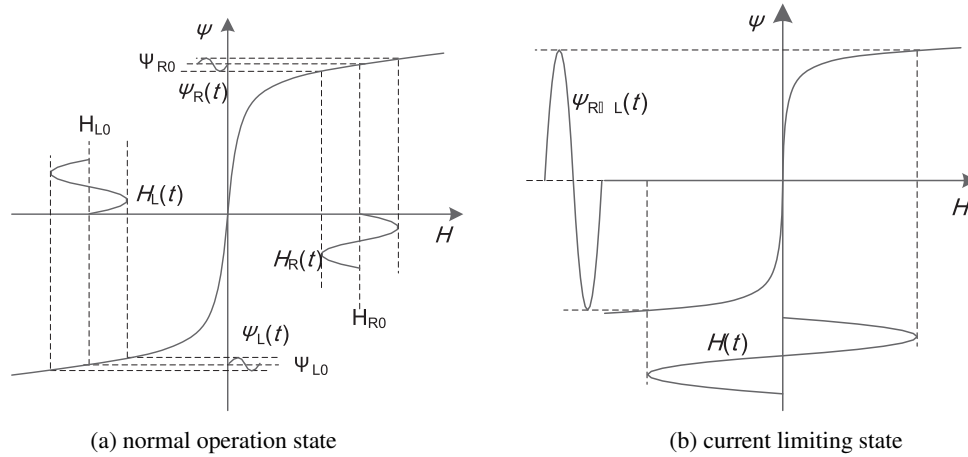


Fig. 2. Magnetic condition of SISFCL in normal and current limiting states

According to Faraday's law of electromagnetic induction, the induction electromotive force on the AC winding is: $e = d\Psi_R(t)/dt$. Due to normal operation, the current is low enough, and the change rate of the integrated flux linkage is low as well. As consequence, the induced voltage on the AC winding is very small when the system works in a steady-state. The AC winding is in low impedance, hardly has any effect on the normal power transmission.

When the TL fails, the fast switch opens to release energy stored in the superconducting magnet in order to reduce the DC excitation rapidly and to quit the saturation state.

As showed in Fig. 2(b), $(0, 0)$ is the work point of the left and right iron core. The induced electromotive force of the AC winding is $e = d\Psi(t)/dt$. For the fault current, it usually dozen times the normal current, therefore, the AC winding has an enormous induction voltage. The AC winding is in a high impedance state and is able to limit short-circuit current.

When the SISFCL is connected to the TL, it can be considered as a current controlled voltage source:

$$\begin{cases} U = e + L \frac{di}{dt} + Ri \\ \frac{d\Psi(t)}{dt} = NS \frac{dB}{dt} \\ Ni = Hl \end{cases} \quad (1)$$

The voltage current relationship of the SISFCL can be obtained by Formula (1):

$$U = \left(\frac{N^2 S}{l} \frac{dB}{dH} + L \right) \frac{di}{dt} + Ri, \quad (2)$$

where: e is the induced electromotive force for the AC winding, L is the leakage inductance of the AC winding, R is the resistance of the AC winding, Ψ is the flux linkage of the AC core, N is the number of turns of the AC winding, S is the cross-sectional area of the AC core, B stands for the magnetic flux density of the iron core, H is the magnetic field strength of the AC iron, l is the effective path length.

2.2. The principle of distance protection

Due to the characteristics of fast response and high selectivity of DP, it has been widely deployed in the protection system of high voltage TL. The main component of the DP is an impedance relay. The measured impedance is utilized to reflect the distance from the installation point to the short-circuit point.

The faulty section of the TL is located by measuring the voltage and current of the transformer, calculating the impedance Z_m and compared with the setting impedance Z_{set} . The action signal is given as $Z_m < Z_{set}$, otherwise, the action signal is not granted.

The directional circle is part of the most applied characteristics in the operation of various impedance relays. Fig. 3 is the operation characteristic of section I and II, and the setting impedances are:

$$\begin{cases} Z_{set,1}^I = K^I Z_{AB} \\ Z_{set,1}^{II} = K^{II} (Z_{AB} + Z_{set,1}^I) \end{cases}, \quad (3)$$

where: $Z_{set,1}^I$ and $Z_{set,1}^{II}$ are the setting impedances of the first point in DP section I and II, $Z_{set,2}^I$ is the setting value of the second point in DP section I, K^I and K^{II} are respectively the reliability coefficients of DP section I and II, $K^I = 0.8 \sim 0.85$, $K^{II} = 0.8$, Z_{AB} is the positive sequence impedance of the total fundamental line.

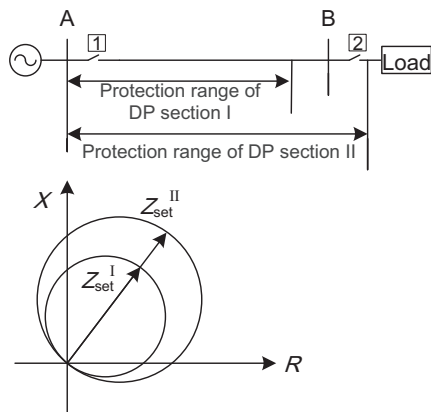


Fig. 3. Operation characteristics and protection zone of impedance relay

3. The impact of SISFCL on the TL protection

As showed in Fig. 4, for the TL with the SISFCL, (SISFCL is connected within I and II section of TLDP). k is the fault point of the TL.

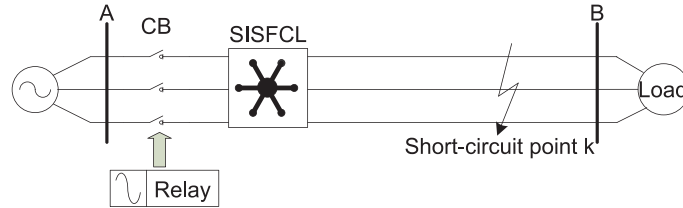


Fig. 4. The topology of the transmission line with SISFCL

3.1. The impact of SISFCL on ground distance protection

When the TL is subjected to a three-phase or two-phase ground fault, it can be considered as three or two single-phase grounding faults. When a single-phase metal grounding short-circuit fault has occurred to the line, take phase A as an example:

$$\begin{cases} \dot{U}_A = (\dot{I}_A + 3K\dot{I}_0)z_1l_k \\ Z_m = z_1l_k \frac{\dot{U}_A}{\dot{I}_A + 3K\dot{I}_0} \end{cases}, \quad (4)$$

where: K is the compensation coefficient of the zero-sequence current, I_0 is the zero-sequence current, z_1 is the positive sequence impedance of a line, Z_m is the measured impedance, l_k is the distance from the protection installation point to the short-circuit point k . When the SISFCL is connected to TL, the Z_m can correctly reflect the l_k in the zero-sequence current compensation state.

When the SISFCL is connected to the TL, the following illustration is based on phase A:

$$\begin{cases} \dot{U}_A = (\dot{I}_A + 3K\dot{I}_0)z_1l_k + \dot{I}_AZ_{\text{sfc1}_A} \\ \frac{\dot{U}_A}{\dot{I}_A + 3K\dot{I}_0} = Z_m + \frac{\dot{I}_A}{\dot{I}_A + 3K\dot{I}_0}Z_{\text{sfc1}_A} = Z_m + \beta Z_{\text{sfc1}_A} = Z'_m \end{cases}, \quad (5)$$

where: Z_{sfc1_A} is impedance of current limiter; Z'_m is the measured impedance after current limiter connected. It can be seen from (5) that the impedance Z'_m cannot correctly reflect l_k when current limiter is connected to TL.

3.2. The impact of SISFCL on phase distance protection

When a three-phase fault occurs in the TL, the system is still symmetrical, and can be treated as two-phase faults. When a short-circuit fault occurs in two-phase, the AB phase is:

$$\begin{cases} \dot{U}_A = \dot{U}_k + (\dot{I}_A + 3K\dot{I}_0)z_1l_k \\ \dot{U}_B = \dot{U}_k + (\dot{I}_B + 3K\dot{I}_0)z_1l_k \\ \frac{\dot{U}_A - \dot{U}_B}{\dot{I}_A - \dot{I}_B} = z_1l_k = Z_m \end{cases}. \quad (6)$$

The measured impedance Z_m correctly reflects l_k . When the SISFCL is connected to the TL, the AB phase is taken as an example:

$$\begin{cases} \dot{U}_A = \dot{U}_k + (\dot{I}_A + 3KI_0)z_1 l_k + \dot{I}_A Z_{\text{sfcl}_A} \\ \dot{U}_B = \dot{U}_k + (\dot{I}_B + 3KI_0)z_1 l_k + \dot{I}_B Z_{\text{sfcl}_B} \\ \dot{U}_A - \dot{U}_B = (\dot{I}_A - \dot{I}_B)Z_m + \dot{I}_A Z_{\text{sfcl}_A} - \dot{I}_B Z_{\text{sfcl}_B} \\ \frac{\dot{U}_A - \dot{U}_B}{\dot{I}_A - \dot{I}_B} = Z_m + \frac{\dot{I}_A}{\dot{I}_A - \dot{I}_B} Z_{\text{sfcl}_A} - \frac{\dot{I}_B}{\dot{I}_A - \dot{I}_B} Z_{\text{sfcl}_B} = Z'_m \end{cases} \quad (7)$$

From (7), the measured impedance Z'_m cannot reflect l_k correctly after the current limiter connected.

As showed in Fig. 5, when SISFCL is connected to the TL, no matter which kind of fault, Z_{sfcl} makes the measured impedance of the impedance relay changed from Z_m to Z'_m , thus changed the selectivity and sensitivity of the DP.

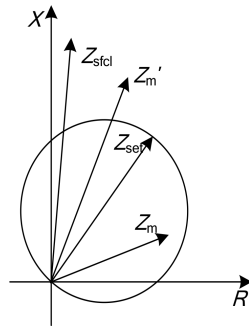


Fig. 5. Impact of SISFCL on measured impedance

4. The improved methods for TL protection

For TL with SISFCL, the measured impedance cannot correctly reflect the fault distance no matter grounding fault or short-circuit fault, when the TL is protected from the original distance and the wiring mode remains unchanged. Therefore, this paper proposed two theoretically feasible methods for the improvement of DP, and an improved DP setting method.

4.1. Changing the setting impedance in real time

When the TL is short-circuited, the connection mode of zero sequence current compensation is obtained by the Formula (5):

$$Z'_m = Z_m + \beta Z_{\text{sfcl}_A} \quad (8)$$

When the TL has an interphase short-circuit fault, the connection between phase faults can be obtained by Formula (7):

$$\begin{aligned} Z'_m &= Z_m + \gamma Z_{\text{sfcl}_A} + (1 - \gamma) Z_{\text{sfcl}_B}, \\ \gamma &= \frac{\dot{I}_A}{\dot{I}_A - \dot{I}_B}. \end{aligned} \quad (9)$$

Resetting the measured impedance Z'_m can ensure the correct action of DP. The corresponding impedance circle characteristics are shown in Fig. 6. α is the offset vector of real time impedance circle: $\alpha = \beta Z_{\text{sfc1}_A}$ (or $\alpha = \gamma Z_{\text{sfc1}_A} + (1 - \gamma) Z_{\text{sfc1}_B}$), Z'_{set} is the real time setting impedance.

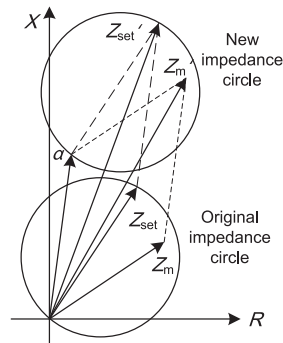


Fig. 6. The characteristics of the impedance circle before and after changing the setting impedance

4.2. Changing the connection mode

When the ground short-circuit fault occurred to the TL, from Formula (3) can be obtained as:

$$\frac{\dot{U}_A - \dot{I}_A Z_{\text{sfc1}_A}}{\dot{I}_A + 3K \dot{I}_0} = z_1 l_k. \quad (10)$$

When the TL has an interphase short-circuit fault, the transformation of (7) can be obtained:

$$\frac{\dot{U}_A - \dot{U}_B - \dot{I}_A Z_{\text{sfc1}_A} + \dot{I}_B Z_{\text{sfc1}_B}}{\dot{I}_A - \dot{I}_B} = z_1 l_k. \quad (11)$$

We assumed the voltage and the current of the ground-fault impedance relay are added to $\dot{U}_A - \dot{I}_A Z_{\text{sfc1}_A}$ and $\dot{I}_A + 3K \dot{I}_0$ respectively, and the voltage and the current of the phase-fault impedance relay are added to $\dot{U}_A - \dot{U}_B - \dot{I}_A Z_{\text{sfc1}_A} + \dot{I}_B Z_{\text{sfc1}_B}$ and $\dot{I}_A - \dot{I}_B$ respectively. Formulas (9) and (5), Formulas (11) and (6) have the exact same structure. It means that, by changing the connection mode, the improved DP can reflect the l_k correctly as well as the unequipped situation, and there is no necessary changing the setting impedance Z_{set} of the original DP.

4.3. An improved setting method for DP

As distinct from the resistance type superconducting fault current limiter in [14], instead of a fixed value, the impedance Z_{sfc1} of the SISFCL varies in real time, The magnitude of the impedance is related to the short-circuit current, the number of turns of the AC winding and the structure of the iron core.

The above methods need to calculate the real time limiting impedance Z_{sfc1} of the SISFCL. The impedance of the SISFCL is pulsed type in the current limiter state, thus Z_{sfc1} is not easy to calculate. Therefore, an improved setting method for the DP is proposed in this paper: section I is still adjusted according to 85% of total line impedance, setting section II with enough sensitivity to the terminal fault, section III is set according to the minimum load. Finally, time delay protection is utilized to protect the coordination among all levels of the DP.

The impedance of the SISFCL decreases as the fault current increases. As shown in Fig. 7, when the SISFCL is connected to the TL, the impedance of the first point of section II is set according to the M point of the minimum operating mode.

$$Z_{\text{set},1}^{\text{II}}(1) = K^{\text{II}}(Z_{AB} + Z_{\text{SFCL},M,\text{min}}). \quad (12)$$

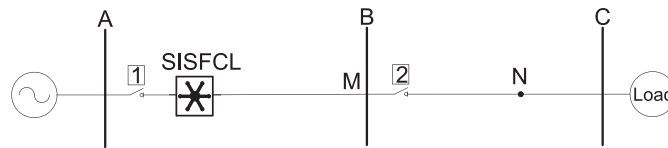


Fig. 7. Re-setting on section II of distance protection

According to the traditional setting method of section II, the setting value of the first point in section II is set according to the short-circuit impedance at the N point at the maximum operating mode, in order to shorten the time delay between section I and II (BN is the protection range from section BC to section I).

$$Z_{\text{set},1}^{\text{II}}(2) = K^{\text{II}}(Z_{AB} + Z_{\text{set},2}^{\text{I}} + Z_{\text{SFCL},N,\text{max}}). \quad (13)$$

In the formula, $Z_{\text{SFCL},N,\text{max}}$ and $Z_{\text{SFCL},M,\text{min}}$ are the impedances of the fault points N and M, when the system is in the maximum and minimum operating modes.

In order to ensure that the distance between section I is longer than that of section II, the protection range must be ensured with $Z_{\text{set},1}^{\text{II}}(1) < Z_{\text{set},1}^{\text{II}}(2)$.

5. Simulation and Analysis

A unilateral power supply system has been built as it is shown in Fig. 4. The simulation parameters are: 230 kV, 50 Hz of A bus voltage. The length of the TL is 60 km, the positive and zero resistance, inductance and capacitance per km are respectively 0.0705 Ω , 1.27 mH, 8.6 nF and 0.323 Ω , 3.822 mH, 6.05 nF.

The DP of grounding fault and phase fault should adopt different types of impedance relay, the setting impedance can be calculated according to the positive sequence impedance. The setting impedance of section I and II are the same ones, so we only do research on the grounding fault protection. To facilitate analysis, make the following hypothesis:

1. The neutral point of the substation is direct grounding.
2. All grounding faults are metal grounding faults.
3. The fault occurred at $t = 0.5$ s.
4. The protective line of DP section I covers 85% of the full length, section II covers the extensive length.

5.1. Analysis on Model and Performance of SISFCL

In this paper, the 220 kV/300 MVA SISFCL of the running test of the substation of Tianjin Shi Gezhuang is taken as the research object. The DC winding is applied with the BSCCO2223 superconducting material. Main parameters of the flow limiter are shown in Table 1. The steel sheet coefficient of DQ130 silicon is 0.97, the B-H curve is shown in Table 2.

Table 1. Parameters of SISFCL model

Parameters	Value
Diameter of AC column D_{AC} (mm)	475
Diameter of DC column D_{DC} (mm)	812.8
Height of inside window H_a (mm)	1180
Width of inside window H_b (mm)	660
Resistance of AC winding $R_g/m\Omega$	19.5
Number of winding turns N_{AC}	60/phase
Ampere turns of DC excitation $F(A)$	110000

Table 2. Relationship of B-H curve of DQ130 silicon steel

B (T)	H (A/m)	B (T)	H (A/m)	B (T)	H (A/m)
0	0	1.52	36	1.94	4000
3	6	1.62	60	1.96	5000
5	8	1.7	120	1.98	7000
8	10	1.8	500	1.99	8000
1.06	13	1.85	1000	2	10000
1.34	20	1.89	2000	2.2	∞

The effective value of the actual transmission current is 500 A, in the steady state operation of the system. Fig. 8 shows the voltage drop at both ends of the SISFCL, its effective value is 2.83 kV, it meets the requirements of a current limiter: in steady-state operation voltage drop is less than 2.5% of the rated voltage.

Fig. 9 shows the short-circuit current simulation of the A grounding fault at the A bus bar at 10 km before and after the SISFCL is connected to the TL.

When the SISFCL is not connected to the TL, the RMS current of short-circuit and the periodic component are respectively 39.61 kA and 22.32 kA. After the SISFCL is connected to the TL, the RMS current of short-circuit and periodic component are respectively 28.01 kA and 16.33 kA, and the short-circuit current is limited by more than 41%.

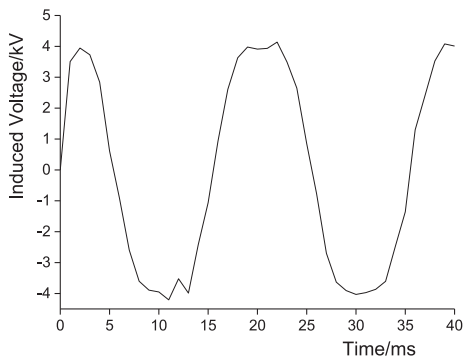


Fig. 8. Voltage drop of current limiter in steady state

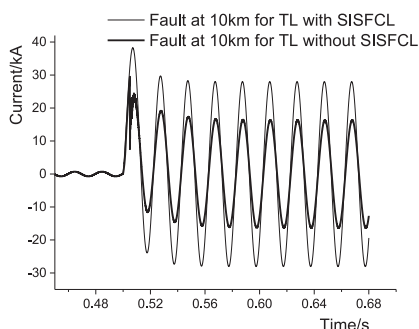


Fig. 9. Single phase short-circuit to ground

5.2. The impact of distance protection with SISFCL

The measured impedance of the TL at 51 km before and after the SISFCL is equipped shown in Fig. 10 when a grounding fault happened. Circle1 is an impedance setting circle for DP section I. Curve1 is the measured impedance before the SISFCL is connected to the TL. As it can be observed from Fig. 8, the DP can protect 85% of the total length, which accords with the theoretical requirements. Curve2 is the measured impedance after the SISFCL is connected to the TL, which refers to the access of the results in the reduced range of DP section I. Only 75% of the total length can be protected.

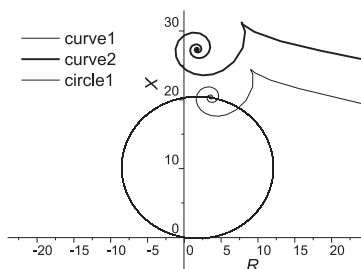


Fig. 10. Measured impedance in single phase short-circuit to ground

curve1/curve2 in Fig. 11 are the action signals issued by the relay before/after the SISFCL is equipped. As it can be seen, 20 ms after the fault occurred (curve1), the relay sent an action

signal. 22 ms after the fault occurred (curve2), the relay sends an action signal. Therefore, the equipment of the SISFCL has an influence on the selectivity and sensitivity of DP section I. The influence of section II is similar to that of section I.

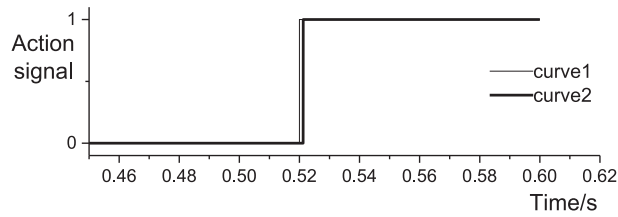


Fig. 11. Action signal in single phase short-circuit to ground

5.3. Re-setting of distance protection

Table 1 shows the limiting impedance of the SISFCL, when the system in the minimum and maximum operational mode at different fault locations. Taking the simulation parameters in Table 3 into Formulas (10), (11), it turns out that $Z_{set,1}^{II}(1) < Z_{set,1}^{II}(2)$. Setting the impedance of section I as with $Z_{set,1}^{II}(1)$ can guarantee the sensitivity of M fault within section II, even shorten the cooperation time delay of point 2 to section I.

Table 3. The changes of the impedance in SISFCL with the fault point

Location of the fault from the bus A (km)	10	30	50	M point	N point
The SISFCL impedance in minimum operating mode (Ω)	4.61	5.24	5.81	6.09	–
The SISFCL impedance in maximum operating mode (Ω)	–	–	–	–	5.34

Fig. 12 shows the relationship between an impedance circle and measurement impedance in section II of the DP: Curve1 is the measured impedance of single phase grounding fault at the end of the TL. Circle1 is the impedance circle of DP section II of the new setting method. As shown, DP section II can protect the full length.

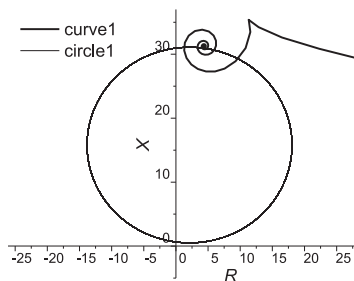


Fig. 12. E-adjusted impedance of DP in section II

Fig. 13 is the action signal of the DP section II at the end of the TL under the single phase grounding fault after the resetting of the impedance: 20 ms after the fault had occurred, the relay sent an action signal, which means that the DP was sufficiently sensitive to the end of the TL.

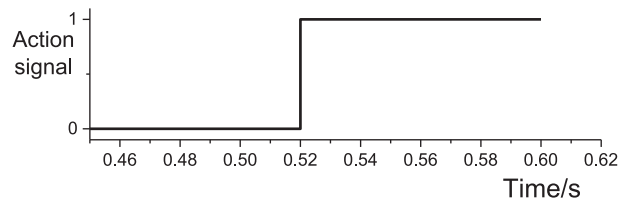


Fig. 13. Action signal at the end of the fault after re-adjusting the impedance of DP in section II

6. Conclusion

This paper utilized the working principles of the SISFCL and DP to build a 220 kV current limiter, DP and transmission network models. Through theoretical analysis and simulations, the conclusions are drawn as follows:

1. The SISFCL can limit short-circuit current more than 40% when a short-circuit fault occurs, in order to minimize the impacts on the primary equipment such as a circuit breaker.
2. With the increase of the distance between the fault point k and the A bus, the impedance of the SISFCL also increases, and affects the selectivity and sensitivity of the DP.
3. The setting method, proposed in this paper, can effectively reduce the influence of a current limiter on the TLDP by recalculating the setting value of the distance of section II. This study was carried out to provide certain references for the application of the SISFCL in the TL.

Acknowledgement

This work was supported by the Natural Science Foundation of China (61461023) and by the Natural Science Foundation of Gansu Province, China (2016GS07210).

References

- [1] Sarkar D., Upadhyaya A., Choudhury A.B. et al., *Investigation of the performance of SISFCL with the variation of hysteretic characteristics*, 2015 Annual IEEE India Conference (INDICON), New Delhi, India, pp. 1–5 (2015).
- [2] Jia Y.L., Mark D.A., Hu D. et al., *Numerical Simulation and Analysis of a Saturated-Core-Type Superconducting Fault Current Limiter*, IEEE Transactions on Applied Superconductivity, vol. 27, no. 4, pp. 1–5 (2017).
- [3] Wei Z.Q., Xin Y., Jin J.X. et al., *Optimized Design of Coils and Iron Cores for a Saturated Iron Core Superconducting Fault Current Limiter*, IEEE Transactions on Applied Superconductivity, vol. 26, no. 7, pp. 1–4 (2016).

- [4] Bock J., Hobl A., Schramm J. et al., *Resistive superconducting fault current limiters are becoming a mature technology*, IEEE Transactions on Applied Superconductivity, vol. 25, no. 3, pp. 1–4 (2015).
- [5] Vilhena N., Taillacq A., Pronto A. et al., *Analysis of Electromagnetic Forces in Superconducting Fault-Current Limiters Under Short-Circuit Condition*, IEEE Transactions on Applied Superconductivity, vol. 26, no. 3, pp. 1–4 (2016).
- [6] Jia Y.L., Shi Z.J., Zhu H.J. et al., *Cognition on the Current-Limiting Effect of Saturated-Core Superconducting Fault Current Limiter*, IEEE Transactions on Magnetics, vol. 51, no. 11, pp. 1–4 (2015).
- [7] Hong H., Su B., Niu G.J. et al., *Design, Fabrication, and Operation of the Cryogenic System for a 220 kV/300 MVA Saturated Iron-Core Superconducting Fault Current Limiter*, IEEE Transactions on Applied Superconductivity, vol. 24, no. 5, pp. 1–4 (2014).
- [8] Upadhyaya A., Sarkar D., Choudhury A.B. et al., *Performance analysis of a three-phase SISFCL with the variation of circuit parameters using jiles atherton hysteresis model*, 2016 2nd International Conference on Control, Instrumentation, Energy & Communication (CIEC), Kolkata, India, pp. 220–224 (2016).
- [9] Pellecchia A., Klaus D., Masullo G. et al., *Development of a Saturated Core Fault Current Limiter With Open Magnetic Cores and Magnesium Diboride Saturating Coils*, IEEE Transactions on Applied Superconductivity, vol. 27, no. 4, pp. 1–7 (2017).
- [10] Xin Y., Hong H., Wang J.Z. et al., *Performance of the 35 kV/90 MVA SFCL in Live-Grid Fault Current Limiting Tests*, IEEE Transactions on Applied Superconductivity, vol. 21, no. 3, pp. 1294–1297 (2011).
- [11] Xin Y., Gong W.Z., Sun Y.W. et al., *Factory and Field Tests of a 220 kV/300 MVA Saturated Iron-Core Superconducting Fault Current Limiter*, IEEE Transactions on Applied Superconductivity, vol. 23, no. 3, p. 5602305 (2013).
- [12] Hong H., Cao Z.J., Zhang J.Y. et al., *DC Magnetization System for a 35 kV/90 MVA Superconducting Saturated Iron-Core Fault Current Limiter*, IEEE Transactions on Applied Superconductivity, vol. 19, no. 3, pp. 1851–1854 (2009).
- [13] Liu H.L., Jiang D.Z., Chen G. et al., *Improved Setting Method of Distance Protection with the SSFCL*, Automation of Electric Power System, vol. 30, no. 2, pp. 90–95 (2006).
- [14] Liu B., Mei J., Zheng J.Y. et al., *Improved Distance Protection Setting Method for the Single-Phase Ground Fault with Grid-Connected SFCL*, East China Electric Power, vol. 40, no. 5, pp. 793–798 (2012).
- [15] Li B., Li C., Guo F.R., *Application Studies on the Active SISFCL in Electric Transmission System and Its Impact on Line Distance Protection*, IEEE Transactions on Applied Superconductivity, vol. 25, no. 2, pp. 1–9 (2015).